A thermokinetic model of complex oscillations in gaseous hydrocarbon oxidation

Xiao-jing Wang and Chung Yuan Mou[a)]
Faculté des sciences, Université Libre de Bruxelles, Campus Plaine, C. P. 231, Bd. du Triomphe, B-1050 Bruxelles, Belgium

(Received 21 February 1985; accepted 16 May 1985)

A three variable thermokinetic model of ignition is devised to describe the gas-phase oxidation of hydrocarbons in CSTR. For a single set of thermokinetic parameters, the model displays steady states, bistability, cool flame oscillation, simple ignition oscillation, and complex ignition-cool flame oscillations, when the reactant pressure P and vessel temperature T_0 are varied as control parameters. The predicted P-T_0 state diagram compares fairly well with the experimental finding for the system of acetaldehyde/oxygen. The model also predicts interesting bifurcation sequences of complex periodic states. The proposed skeleton model is justified qualitatively by considering detailed kinetics in the oxidation of acetaldehyde.

I. INTRODUCTION

Recently, some interesting experimental studies have been carried out on the spontaneous gas-phase oxidation of hydrocarbon and related fuels in far-from-equilibrium situations. In an equimolar mixture of acetaldehyde and oxygen in a continuous-flow stirred tank reactor (CSTR) for instance, a remarkable variety of dynamic behaviors—steady states, bistability, cool flame oscillation, ignition oscillation, and complex ignition-cool flame oscillations—were observed when external control parameters, such as reactant pressure and vessel temperature, were varied.[1] The investigation of such phenomena is important not only for the obvious reason of understanding the ignition process and its possible practical implications such as in the problem of engine knock[2]; but more fundamentally, it provides a new family of chemical systems, of thermokinetic origin, that will broaden our horizon on chemical instabilities[3] and nonlinear dynamic phenomena.[4]

Up to now, the best known chemical systems exhibiting complex dynamics are isothermal so that temperature does not play a significant role.[5] A remarkable and intensively studied example is the Belousov–Zhabotinskii reaction, the modeling of which is based essentially on a simple kinetic scheme with three nonlinearly coupled components, called the Oregonator.[6]

In the case of the oxidation of hydrocarbon fuels, there are two sources of dynamical complexity. First, in exothermic reactions, temperature becomes an essential dynamical variable and is coupled with other chemical variables owing to the Arrhenius law of rate coefficients. Second, there are autocatalytic chain-branching mechanisms involving many elementary reactions. One can write down more than 20 elementary steps even for the simplest system, methane/oxygen.

A detailed knowledge of elementary kinetic steps is necessary for a complete understanding of the whole process. Halstead *et al.*[7,8] have analyzed available kinetic data and modeled the acetaldehyde oxidation in a closed system. By recognizing the reaction cycles, chain branchings, and termination steps, they established a model with seven variables, and simplified it to a three variable system using some quasisteady state approximations. The latter model, studied further by Felton *et al.*[9] for an open system, is able to describe oscillatory cool flames, but not oscillatory ignitions. Recently, Gibson *et al.*[10] considered a kinetic model involving 25 reactions, and their numerical simulation gives spontaneous complex ignition-cool flame oscillations.

These detailed analyses, however, did not furnish a simple theoretical framework for a fundamental understanding of those complex dynamic behaviors mentioned at the beginning of this section.[1] A more synthetic view is needed.

Phenomenologically speaking, cool flames are a mode of hydrocarbon combustion which is associated with a temperature rise of about 100 K and small fuel consumption. They were recognized as early as the last century,[11] and seem to be widespread in the combustion of many alkanes, alkenes, and their oxygenated derivatives.

Contrary to a cool flame, ignition is a violent event accompanied by bright light pulses during which the temperature rises more than 500 K while oxygen and fuels are almost depleted. When the ignition process is followed closely, two stages are distinguishable: The first, as precursor, shares all characteristics of a cool flame, and the second is an explosive change. For a CSTR system, oscillatory ignition is possible, sustained by the continuous inflow of reactants.

Cool flame oscillation was satisfactorily modeled more than ten years ago by Gray and Yang.[12] They combined a chain-branching mechanism with the thermokinetic approach of Salnikoff,[13] and proposed a dynamic system with two variables (autocatalytic chain carrier and temperature)

$$A \xrightarrow{k_i} X, \text{ initiation}$$

$$X \xrightarrow{k_b} 2X, \text{ branching}$$

$$\left.\begin{aligned} X &\xrightarrow{k_{t_1}} \text{stable products} \\ X &\xrightarrow{k_{t_2}} \text{stable products} \end{aligned}\right\} \text{termination},$$

[a] Permanent address: Department of Chemistry, National Taiwan University, Taipei, Taiwan 107.

 0021-9606/85/214554-08$02.10

where concentration and temperature were considered as spatially uniform, and a constant concentration of A was assumed. This model combines two instability features, self-heating and chain branching, in a single scheme. There are two termination steps and, as the activation energies are assumed to satisfy the inequality $E_{t_1} > E_b > E_{t_2}$, self-heating is counteracted by the high temperature termination. Steady states and cool flame oscillations were all predicted by the model in a complicated P–T_0 state diagram, cool flame oscillation being located in the region of the negative temperature coefficient effect.

However, the Gray–Yang model is definitely unable to describe oscillatory ignition and complex oscillations where oscillatory ignitions are interspersed by cool flames. A simple, though perhaps superficial, reason for this failure is that such complex dynamic behaviors are topologically forbidden on a plane, thus indicating that two variables are not sufficient.

The purpose of the present work is to investigate the simplest kinetic features of hydrocarbon oxidation, and to propose a model of ignition, which also contains the mechanism of cool flame because of the two-stage feature of the ignition, and consequently provides a theoretical basis of explaining various complex oscillations observed in such systems.

We first present (in Sec. II) a skeleton model of the oxidation of hydrocarbons which originates from the Gray–Yang model. The essential modifications are twofold: The fuel and oxygen are treated as temporal variables and the system is considered in CSTR condition; a new high temperature chain-branching mechanism is added.

In Sec. III, numerical simulations based on our model are reported. They lead to the characteristic two-stage ignition in addition to steady states and cool flame oscillation. The constructed P–T_0 state diagram compares well qualitatively with experiment. In particular, interesting bifurcation sequences of complex oscillations in which the number of cool flames between two ignition peaks increases in a peculiar way are observed.

A discussion of the relationship between the proposed model and the detailed chemical kinetics constitutes the subject of Sec. IV.

Finally, in Sec. V we give a brief discussion of the results of this modeling and their implications.

II. THERMOKINETIC MODEL

The proposed scheme is as follows:

$$Y \xrightarrow{k_1} X, \tag{1}$$

$$X + Y \xrightarrow{k_2} fX, \tag{2}$$

$$X \xrightarrow{k_3} 2X, \tag{3}$$

$$X \xrightarrow{k_4} S_1, \tag{4}$$

$$X \xrightarrow{k_5} S_2, \tag{5}$$

where the concentrations of fuel and oxygen, assumed to be equal, are represented by Y; X denotes the autocatalytic chain carrier to be identified in Sec. IV, and f is a suitable stoichiometric coefficient greater than unity. h_i is the heat of the ith reaction step. The rate constants k_i are of Arrhenius form with activation energies E_i.

Step (1) is merely the initiation mechanism and step (5) the low temperature termination; while steps (3) and (4), chain-branching and high temperature termination, respectively, play a more crucial role in the scheme. To model oscillatory cool flames, one requires that $E_4 > E_3 > E_5$. If we look at the temporal evolution of cool flame oscillation, the chain-branching step (3) dominates initially when the temperature of the system starts rising. This reaction step generates heat and enhances thereby its own rate in an exponential fashion. As the temperature rises, a moment must come when the high temperature termination (4), which is exothermic, becomes dominant. X then decreases so that the temperature finally cannot continue to increase and falls by the heat loss to the external world. When the temperature decreases to sufficiently low level so that step (4) ceases to have an edge on step (3) the cycle may start over again. This is the essence of the Gray–Yang model, which can be recovered from our model by setting $Y =$ constant and $k_2 = 0$.

In order to model the ignition, fuel and oxygen must be treated as temporally varying, and a third variable Y must be introduced in step (1) and step (2). Moreover, we introduce a new, high temperature chain-branching (2) with activation energy satisfing $E_2 > E_1 > E_4 > E_3 > E_5$, which releases a great amount of heat and rapidly consumes fuel and oxygen. This mechanism is expected to be at the heart of ignition.

Step (2) is coupled to steps (3) and (4) partly through the temperature. In fact, E_2 is so high that step (2) would never be important if steps (3) and (4) did not generate enough heat.

The reason why Y is present in step (2) but not in step (3) is that we expect, as suggested by experiment, that in the cool flame region the consumption of Y is not great. This is merely a convenient simplification.

Let us assume that thermal coupling of the system with the external world can be represented by a Newtonian heat loss term; and that the material flow term is characterized by a residence term $\tau = 1/k_f$. For simplicity, we take $f = 2$, the mass balance and energy balance equations can then be written as

$$\frac{d\tilde{x}}{d\tilde{t}} = \tilde{k}_1 \tilde{y} - (\tilde{k}_4 + \tilde{k}_5 - \tilde{k}_3)\tilde{x} + \tilde{k}_2 \tilde{x}\tilde{y} - k_f \tilde{x}, \tag{6}$$

$$\frac{d\tilde{y}}{d\tilde{t}} = -\tilde{k}_1 \tilde{y} - \tilde{k}_2 \tilde{x}\tilde{y} - k_f(\tilde{y} - y_0), \tag{7}$$

$$C\frac{d\tilde{T}}{d\tilde{t}} = \tilde{k}_1 \tilde{y}\,\tilde{h}_1 + (\tilde{k}_2 \tilde{h}_2 \tilde{y} + \tilde{k}_3 \tilde{h}_3 + \tilde{k}_4 \tilde{h}_4 + \tilde{k}_5 \tilde{h}_5)\tilde{x} - \tilde{k}_T(\tilde{T} - T_0), \tag{8}$$

where C is the specific heat of the system.

After introducing the dimensionless variables

$$x = \frac{\tilde{x}}{y_0}; \quad y = \frac{\tilde{y}}{y_0}; \quad u = \frac{\tilde{T} - T_0}{T_0}; \quad t = k_f \tilde{t};$$

$$k_2 = \frac{\tilde{k}_2 y_0}{k_f}; \quad k_j = \frac{\tilde{k}_j}{k_f}\,(j \neq 2); \quad h_j = \frac{\tilde{h}_j y_0}{T_0 C}; \quad k_T = \frac{\tilde{k}_T}{C k_f}.$$

Equations (6)–(8) become

$$\dot{x} = k_1 y + k_2 xy - (k_4 + k_5 - k_3)x - x, \tag{9}$$

$$\dot{y} = -k_1 y - k_2 xy + 1 - y, \tag{10}$$

$$\dot{u} = k_1 h_1 y + (k_2 h_2 y + k_3 h_3 + k_4 h_4 + k_5 h_5)x - k_T u. \tag{11}$$

The numerical values of the kinetic parameters we used are listed in Table I. A majority of these values are taken from Yang and Gray.[12] Those which are new, i.e., E_2, A_2, and h_2, concern only step (2). The choice of E_2 has already been discussed previously. For h_2, we chose a value roughly four times that of h_4. As to A_2, it was estimated to be large enough so that step (2) can be activated by steps (3) and (4) but not so large so that the ignition occurs too easily, at a temperature for which step (4) is not yet fully activated, thus masking the two-stage character of the process.

We remark that step (5) is a wall termination reaction with $E_5 = 0$; and k_5 is determined by diffusion, dependent on the diameter of reactor d. We set $d = 4$ cm.

The control parameters are reactant pressure P, ambient temperature T_0, and residence time τ. N_0 is the initial total reactant density $N_0 = P/RT_0$. The specific heat of the mixture C is assumed to be constant $C = 11\,N_0$. With respect to the equal fuel/oxygen constitution of the inflow, we choose y_0 to be equal to one-half of the concentration of inflow reactants $y_0 = N_0/2$.

III. SIMULATIONS

To test the model presented in Sec. II, we carried out numerical integrations of the system of ordinary differential Eqs. (9)–(11), using an algorithm of the NAG library based on Gear method. This method was developed especially for stiff ODE systems such as ours. In what follows we choose for the residence time a fixed value $\tau = 4$ s though τ could very well be treated as a varying control parameter like P and T_0.

A. Two-stage ignition

Figure 1 shows a typical oscillation of two-stage ignition, in which the temporal variations of x and u are overlapped in order to see closely how one can understand the underlying mechanism by the aid of the kinetic scheme [steps (1)–(5)]. We see that the first stage of the temperature rise is essentially due to the high temperature termination (4), accompanied by a decrease of x. At the second stage, the high temperature chain branching (2) leads to an abrupt rise of temperature and consumption of y. Moreover, it implies a second peak of x, which is quite sharp but of small amplitude; this is because step (4) which destroys x, turns out to be dominant again as soon as step (2) becomes inactive due to the lack of y.

B. State diagram on P–T_0 plane

In agreement with experimental observations,[1] five distinct types of asymptotic dynamic states (attractors) have been identified in our simulations:

I. Steady state (a stable node) (steady reaction with low T).

II. Relaxation oscillations (oscillatory two-stage ignitions).

III. Complex oscillations (oscillatory ignitions interspersed by cool flames).

IV. Smooth oscillations (oscillatory cool flames).

V. Steady state (a stable focus) (steady reaction with moderately high T).

Figure 2 gives the state diagram which shows the location of these states in the P–T_0 plane.

In Fig. 3, we give three illustrations of the temporal evolution of the temperature chosen from Fig. 2. The behaviors are strikingly similar to the experimental observations of Gray *et al.*[1]

To see the transitions between these various states, it is convenient to fix the value of P, and then to start in region V and proceed from the high T_0 regime to the low T_0 regime. The transition from region V to region IV is a Hopf bifurcation; the period of the limit cycle increases as T_0 decreases towards region III. Both regions V and IV share the negative temperature coefficient effect in that the mean temperature of the system and the rate of heat release increase for decreasing T_0.

The underlying dynamics of the transitions from region IV to region III and from region III to region II have not yet been clarified, although one may intuitively argue that, for the former, ignitions occur because the maxima of the oscillatory cool flame attain a certain threshold; and for the latter, that these maxima are so high that every cool flame without exception leads to an ignition. As to the transition between regions II and I, we observe that the period of relaxation oscillation (the induction time of ignition) becomes larger and larger as this boundary is approached from the right. Numerical evidence makes us suspect that this period actually tends to infinity at the boundary, indicating that this bifurcation might result from a collision of the relaxation oscillation limit cycle with a fixed point of saddle type. This

TABLE I. Thermokinetic parameters used in Eqs. (6)–(8).

$\tilde{k}_1(\mathrm{s}^{-1}) = A_1 N_0 e^{-E_1/R\tilde{T}}$	$A_1 = 1.6\times10^{10}$	$E_1 = 24$ (kcal mol^{-1})	$\tilde{h}_1 = 0$
$\tilde{k}_2(\mathrm{mol}^{-1}\,\mathrm{cm}^3\,\mathrm{s}^{-1}) = A_2 e^{-E_2/R\tilde{T}}$	$A_2 = 3.7\times10^{12}$	$E_2 = 25$ (kcal mol^{-1})	$\tilde{h}_2 = 92$ (kcal mol^{-1})
$\tilde{k}_3(\mathrm{s}^{-1}) = A_3 N_0 e^{-E_3/R\tilde{T}}$	$A_3 = 1.38\times10^{8}$	$E_3 = 7$ (kcal mol^{-1})	$\tilde{h}_3 = 4$ (kcal mol^{-1})
$\tilde{k}_4(\mathrm{s}^{-1}) = A_4 N_0 e^{-E_4/R\tilde{T}}$	$A_4 = 7.8\times10^{10}$	$E_4 = 16$ (kcal mol^{-1})	$\tilde{h}_4 = 20$ (kcal mol^{-1})
$\tilde{k}_5(\mathrm{s}^{-1}) = A_5 N_0^{1/2}/d$	$A_5 = 3.3\times10^{3}$	$E_5 = 0$	$\tilde{h}_5 = 0$
$\tilde{k}_T$ (cal cm^{-3} K^{-1} s^{-1}) $= 3.68\times10^{-4}$			

N. B. After the rescaling of variables, $\tilde{k}_j = k_{j0}\, e^{-E_j/R\tilde{T}} = k_{j0}\, e^{-\frac{1}{\epsilon_j}\frac{1}{\epsilon_j}\frac{u}{1+u}}$, $\epsilon_j = \dfrac{RT_0}{E_j}$.

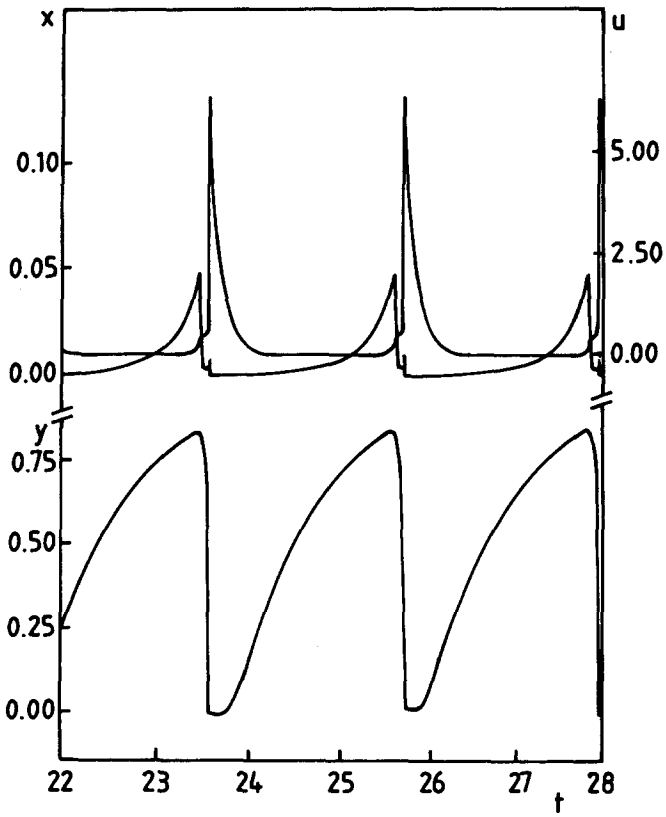

FIG. 1. Oscillation of two-stage ignitions represented by the temporal evolutions of the three components (x, y, u) of the system. $\tau = 4$, $p = 560$, and $T_0 = 580$. Initial condition is $(x, y, u) = (0,1,0)$.

point will be discussed a little more below in connection with bistability phenomena.

Comparing Fig. 2 with the experimental state diagram constructed by Gray *et al.*,[1] qualitative agreement between the two is more than satisfactory. One may notice, however, that the whole experimental diagram is at pressures much

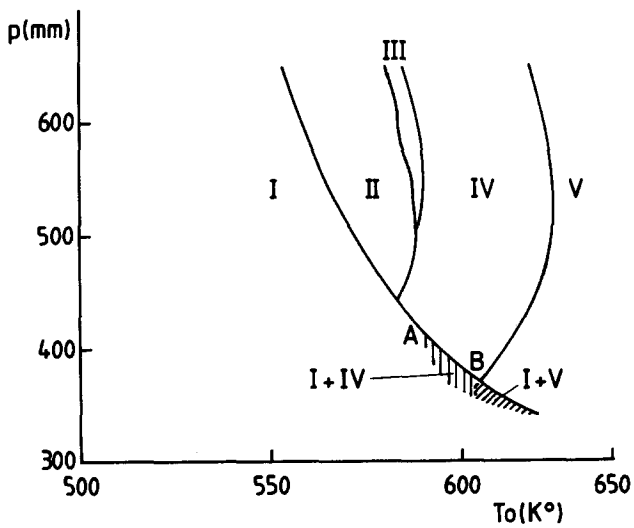

FIG. 2. P–T_0 state diagram constructed for the kinetic parameter values given in Table I, and $\tau = 4$. The I–V regions are explained in the text. The solid boundary lines were drawn by simulations with the initial condition $(x, y, u) = (0,1,0)$; while the dashed area was drawn with other initial conditions and represents bistabilities.

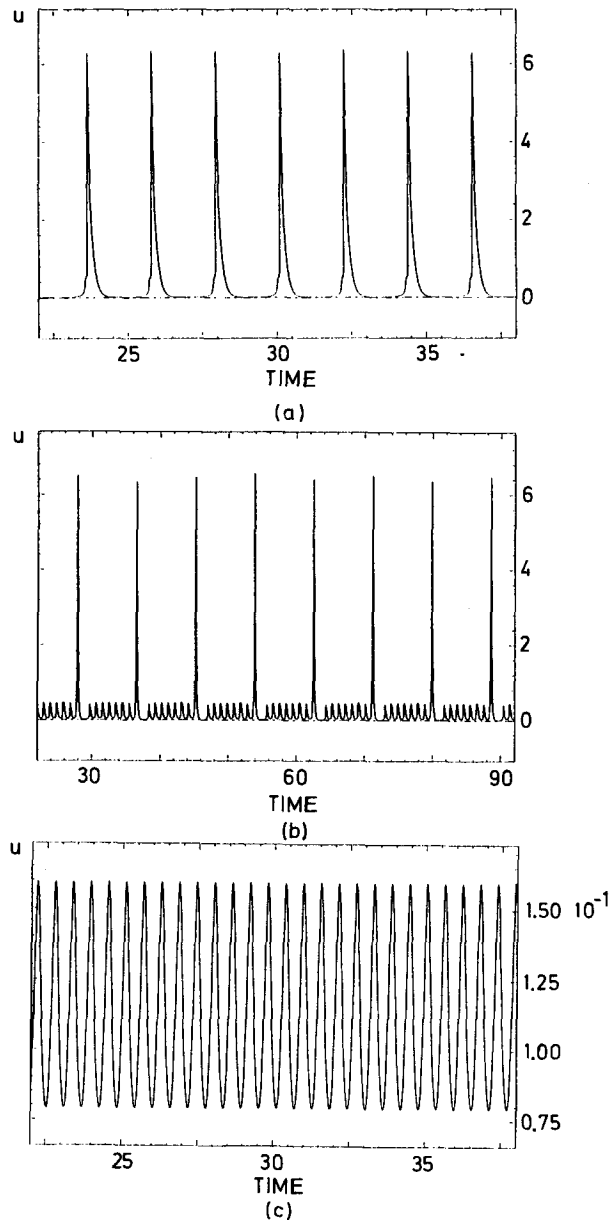

FIG. 3. Three examples of temperal temperature evolution of the system, corresponding respectively to the regions II, III, and IV of Fig. 2. (a) $T_0 = 585$; (b) $T_0 = 589.455$, (c) $T_0 = 620$.

lower than those in Fig. 2. The origin of this shift, we think, is that numerical values of the kinetic parameters used here are appropriate for the oxidation of hydrocarbons capable of generating acetyl radicals, rather than for the acetaldehyde oxidation itself. As will be discussed in Sec. IV, in acetaldehyde oxidation, the low temperature chain branching (3) and high temperature termination (4) would be more efficient than in other cases, while the heat release of step (3) would be less important. For this reason we have constructed another state diagram assuming smaller values of E_3, E_4, and $\tilde{h}_3$, which is shown in Fig. 4. This diagram indeed corresponds to a lower pressure regime.

C. Bistability

If the transition between regions II and I is due to the collision between a limit cycle and a fixed point of saddle

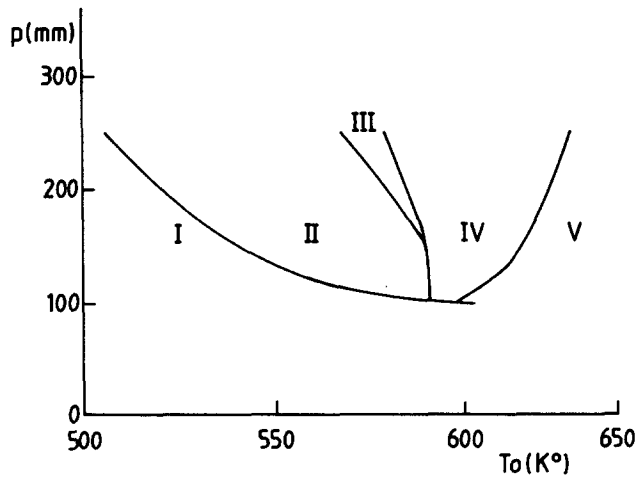

FIG. 4. P–T_0 state diagram constructed in the same way as Fig. 2, but with modified and smaller values of E_3, E_4, and h_4: $E_3 = 6$, $E_4 = 15$, $h_4 = 15$ (kcal). The domain of bistabilities was not drawn here.

type, this collision should be independent of the nodal fixed point arising in region I. Hence, the phenomenon of hysteresis is to be expected, in agreement with what has been seen experimentally.[1]

All the solid boundary lines in Fig. 2 were drawn from integrations of Eqs. (9)–(11) carried out with the same and natural initial condition $(x, y, u) = (0,1,0)$. To probe for bistability and hysteresis, we tried different initial conditions, despite numerical difficulties due to the very large period of oscillation from one side, and the two unknown basins of attractivity for regions I and II, respectively, from the other. But it turns out that in all our simulations no bistability between regions I and II has been identified.

On the other hand, bistability was found at the lower part of the state diagram (below the point A in Fig. 2) both between regions I and IV and between regions I and V. This is indicated by the shaded area in Fig. 2.

The schematic bifurcation diagrams represented in Fig. 5 offer a possible explanation of this. Assume that for a fixed value of pressure, we represent the steady states by u_s as a function of T_0. For T_0 below certain tangent bifurcation point T_{01} there are three steady states. The lowest branch is always stable and corresponds to region I; while the middle branch is of saddle nature. A Hopf bifurcation (T_{02}) occurs on the upper branch V. Moreover, suppose that the transition from region IV or II to I is due to the same mechanism, i.e., caused by an encounter of the limit cycle with that saddle point.

We see from Fig. 2 that the distance between the Hopf bifurcation T_{02} and the tangent bifurcation T_{01} is larger when P is higher. Consequently, one can imagine that, for sufficiently high pressure, the limit cycle issuing from the upper branch V is able to grow large enough for decreasing T_0 to encounter the saddle point almost as soon as this latter appears at T_{01}, together with the lowest branch I. This implies that bistability would be observable only for low pressure, as shown by Figs. 5(a) and 5(b). It indicates also that a suitable modification of the kinetic parameter values could possibly move the point A in Fig. 2 upwards and give rise to bistability of regions I and II.

When the pressure decreases, the Hopf bifurcation point T_{02} moves to still lower T_0, while the tangent bifurcation point T_{01} shifts in the opposite direction. Therefore, a critical value of P (point B in Fig. 2) exists for which these two bifurcations coincide. Below this value, coexistence of regions I and V becomes possible [Fig. 5(c)].

D. Complex oscillations

In the state diagram shown in Fig. 2, most interesting is region III, which actually contains a whole sequence of different periodic states. Let us consider this region more closely for $P_0 = 560$ Torr. If we denote by P_n^m a complex periodic state having $n(m)$ large (small) amplitude oscillations during one period, various P_1^m were observed in our simulations, while no case with $n > 1$ was found. The result is presented in Fig. 6. We notice that a sequence with odd values of m, $m = 1, 3, 5, 7...$ proceeds from left to right, while another sequence with even values of m, $m = 2, 4, 6, 8...$ originates from the other side. The larger the value of m, the narrower the corresponding range of T_0.

There are other complex periodic states near the right end of region III, the order of which seems irregular. An example of P_1^m with m as large as 46 was found at the very edge of the domain. One should notice that the T_0 variation used to construct Fig. 6 was 0.01 K. If one goes to a finer scale, more detailed bifurcation structure might appear and give further clues for the understanding of their global regularities.

Experimentally, P_1^m with m varying from 1 to 5, have been observed,[1] but the order of their occurrence does not seem to have been definitely established. On the other hand, a complex state like $P_1^m + P_1^{m+1}$ was also found near the site where region III vanishes.

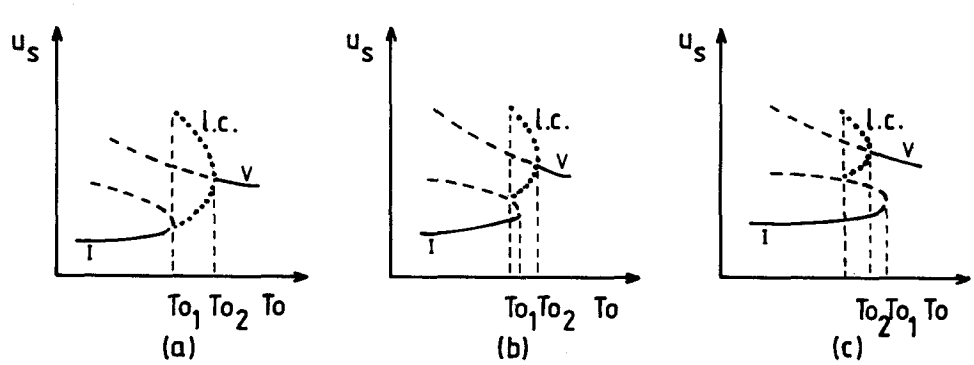

FIG. 5. Schematic bifurcation diagrams for different values of P. (a) $P > P_A$, (b) $P_A > P > P_B$, (c) $P_B > P$ with P_A, P_B corresponding, respectively, to the points A and B in Fig. 2.

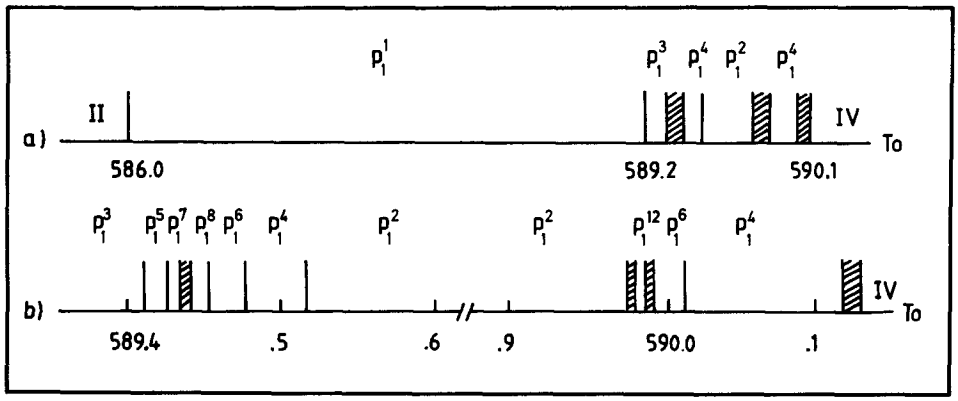

FIG. 6. Bifurcation sequences of complex periodic states found in P–T_0 state diagram (Fig. 2) with $P = 560$. P_1^m denotes a periodic state with m small amplitude oscillations and one large amplitude oscillation per period. The T_0 variations are limited to within 10^{-2} K. (b) is the enlarged picture of one part of (a).

We remark at this point that experimentally, regions II and III seem to meet region I at a single point in the state diagram, in contrast with our case in which it is possible to pass between regions II and IV without crossing region III.

IV. DETAILED MECHANISM FOR OXIDATION OF ACETALDEHYDE

In the last section, we have shown that the proposed skeleton scheme describes well various dynamic behaviors in the oxidation of acetaldehyde. It is natural to inquire whether this skeleton scheme is compatible with detailed kinetics, and what the chemical identity of X is. A deeper understanding of the relationship between the skeleton scheme and detailed kinetics will help us to better estimate the rate constants and heats of reaction in the scheme or lead to further improvement of the scheme itself.

We note that the comparison attempted here can only be qualitative. This skeleton model should not be considered as a straitjacket to fit the currently accepted detail kinetics, but rather as the backbone of it.

Since acetaldehyde oxidation is best understood experimentally, we will mainly examine this system here. Furthermore, the acetyl radical seems to play an important role in degenerate branching in the oxidation of other hydrocarbons capable of generating it.

We will mainly follow the mechanism put forward by Halstead *et al.*[7,8] These authors based their scheme on Blanchard's work,[14] which identified peracetic acid formation and decomposition as the key branching route. We will identify X in our model to be the acetyl radical, which is the precursor of peracetic acid.

A. Initiation

The first step is the generation of acetyl radical

$$CH_3CHO + O_2 \rightarrow CH_3\dot{C}O + H\dot{O}_2. \quad (12)$$

This step is reported to have a high activation energy (170 kJ/mol) and low rate, consistent with its use as our initial step (1). Its low rate also means that the chain carrier CH_3CO cannot have a high concentration at any time.

B. Low temperature branching

The next steps are the formation of peracetic acid from acetyl radical by the low activation energy sequence

$$CH_3\dot{C}O + O_2 \rightarrow CH_3COO\dot{O}, \quad (13)$$

$$CH_3COO\dot{O} + CH_3CHO \rightarrow CH_3COO_2H + CH_3\dot{C}O, \quad (14)$$

$$CH_3COO_2H \rightarrow CH_3COO + \dot{O}H, \quad (15)$$

$$CH_3COO + CH_3CHO \rightarrow CH_3COOH + CH_3\dot{C}O. \quad (16)$$

This sequence gives two acetyl radical for every initial acetyl radical. The last two steps probably have higher activation energies than the first two steps. So the stoichiometric coefficient f in step (3) should be less than 2, but we take $f = 2$ for the sake of simplicity.

C. Termination

Following Yang and Gray,[12] we interpret the low temperature termination step (5) to be the wall destruction of acetyl radical with zero activation energy,

$$CH_3\dot{C}O \rightarrow \text{wall termination}. \quad (17)$$

Another termination mechanism consists of the steps

$$CH_3\dot{C}O + M \rightarrow C\dot{H}_3 + CO + M \quad (18)$$

and

$$2\dot{C}H_3 \rightarrow C_2H_6 \quad (19)$$

and other reactions removing $\dot{C}H_3$ to be identified later. Steps (18) and (19) are the main steps corresponding to high temperature termination in our skeleton model. Step (18) also has a higher activation energy than that of steps (13) and (14) ($E_{18} = 45$ kJ/mol, $E_{13} = 0$, and $E_{14} = 30$ kJ/mol). This is consistent with the requirement of our model. Step (18) by itself is endothermic, but together with later reactions removing $\dot{C}H_3$, the net termination process should be exothermic.

D. High temperature branching

For the purpose of understanding the well known ignition peninsula in the P–T_0 state diagram of aceladehyde oxidation, Halstead *et al.*[7,8] were the first to investigate the detailed underlying kinetics. They pointed out that hydroxyl radical is the important initial species for high temperature chain branching. It can be produced, in addition to step (15), by the following reactions:

$$\dot{C}H_3 + O_2 \rightarrow CH_2O + \dot{O}H, \quad (20)$$

$$CH_3COO_2H \rightarrow \dot{C}H_3 + CO_2 + \dot{O}H. \quad (21)$$

Step (20) is, among the three, the most important one because its activation energy is the lowest.

Hydroxyl radical goes through the following degenerate hydrogen peroxide cycle

$$CH_2O + \dot{O}H \rightarrow \dot{C}HO + H_2O, \quad (22)$$

$$\dot{C}HO + M \rightarrow CO + \dot{H} + M, \quad (23)$$

$$CO + \dot{O}H \rightarrow CO_2 + \dot{H}, \quad (24)$$

$$\dot{H} + O_2 + M \rightarrow \dot{H}O_2 + M, \quad (25)$$

$$\dot{H}O_2 + CH_3CHO \rightarrow CH_3\dot{C}O + H_2O_2, \quad (26)$$

$$H_2O_2 \rightarrow 2\dot{O}H. \quad (27)$$

Of course there are other side reactions involving H, CHO, and HO_2. We write these steps (22)–(27) down to indicate that production of the X species CH_3CO is chain branching in nature through the formation of hydrogen peroxide. This cycle has a much higher activation energy due to the step (27) $E_{27} = 190$ kJ/mol.

HO_2 is also directly formed from the initiation step (12) and gives further formation of acetyl radical in this cycle. But this formation step does not contribute very much except at the very beginning. Most HO_2 will be formed via the CH_3 chain step which is in turn proceeded by the low temperature branching.

To sum up, all the above reactions are organized in Fig. 7 for clarity. The correspondence of our scheme with the detailed kinetics is also summed up in Fig. 7. Note that the set of reactions included in Fig. 7 is by no means complete. In a recent work of Gibson *et al.*,[10] they further take into account the following sequence involving the methyl radical:

$$\dot{C}H_3 + O_2 \rightarrow CH_3\dot{O}_2, \quad (28)$$

$$CH_3\dot{O}_2 \rightarrow \dot{C}H_3 + O_2, \quad (29)$$

$$\dot{C}H_3O_2 + CH_3CHO \rightarrow CH_3O_2H + CH_3\dot{C}O, \quad (30)$$

$$CH_3O_2H \rightarrow CH_3\dot{O} + \dot{O}H \quad (31)$$

by which the chain-branching production of acetyl radical is further enhanced. They believe that steps (28)–(31) are at the heart of cool flame oscillation in acetaldehyde oxidation. From our point of view, both steps (13)–(16) and steps (28)–(31) can provide a low temperature chain branching. But steps (13)–(16) are specific for acetaldehyde while steps (28)–(31) are generally true for many hydrocarbons. The latter is more difficult to be activated than steps (13)–(16) because of the high activation energy of step (31). This would explain the experimental observation that high temperature phenomena in acetaldehyde oxidation occur at much lower pressures than in the oxidation of other hydrocarbons.

Finally, we note that the stoichiometric coefficient for step (3) should probably also be treated as adjustable, in order to reflect the effectiveness of the low temperature chain branching under various conditions.

V. DISCUSSION

In summary, we have presented a simple kinetic model of two-stage ignition which rationalizes the ignition and cool flame in hydrocarbon oxidation, and provides a theoretical framework for the understanding of complex ignition-cool flame oscillations observed experimentally in acetaldehyde oxidation.

One of our two major modifications of the Gray–Yang model, that fuel consumption needs to be taken into account, is quite obvious. The other, i.e., the addition of the high temperature chain branching, is not. In fact, Gonda and Gray[15] recently pursued studies of the original Gray–Yang model to probe whether it is also able to account for two-stage ignition. They found a saddle-type fixed point at high temperature and small x, and argued that an encounter of the limit cycle (of cool flames) with the separatrix of this saddle point would explain the two-stage ignition; the motion of trajectory along the outside of the separatrix corresponding to the "shoulder" of the two-stage ignition. But, it turns out from our preliminary analysis of the steady states, that this saddle fixed point at high temperature does not exist in the system (9)–(11) with the thermokinetic parameter values given in Table I. Therefore, the ignition in our model is necessarily due to a somewhat different mechanism. We intend to report the results of detailed analyses in another communication.

Moreover, complex ignition-cool flame oscillations could not be found in the Gray–Yang model. In another work,[16] Gonda and Gray suggested that these complex oscillations might originate from external fluctuations due to imperfect controls of either temperature or flow. But the present work clearly shows that the existence of region III does not require any external cause. Rather it is due to the intrinsic mechanism of the system. The more detailed simulations by Gibson *et al.*[10] also confirm this point.

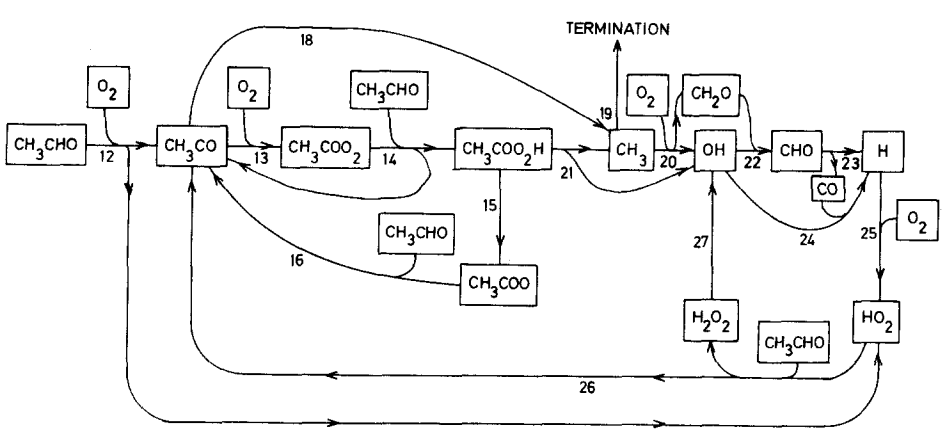

FIG. 7. Schematic diagram of the reaction cycle for the acetaldehyde oxidation. The numbers correspond to the reaction steps in Sec. IV. These reaction steps may be regrouped with respect to the skeleton model (1)–(5): (1) initiation {12}, (2) high temperature branching {18, 20, 22, 23, 24, 25, 26, 27, 15, 21, 12}, (3) low temperature branching {13, 14, 15, 16}, and (4) high temperature termination {18, 19}.

The model presented in this paper is still simple enough to allow a more detailed mathematical analysis to be carried out. On the other hand, it has a large number of thermokinetic parameters, a complete search in parameters space is not feasible, and a sensitivity analysis[17] of this model may be helpful in this respect.

In the future, much attention should be paid to region III of complex oscillations, for which a number of questions may arise. What is the nature of the transition from region IV to region III? Are those two bifurcation sequences with odd and even m, respectively, finite or infinite? What are their dynamic origin and global characteristics? Do the observed periodic states bifurcate from one to another directly, or are some of them "windows" interspersed by still finer cascading structures and even chaotic solutions?

It is noteworthy that in the Belousov–Zhabotinskii reaction bifurcation sequences of periodic states have been observed both for $n = 1$ and $n > 1$[18,19] as well as chaotic states arising from a periodic-doubling sequence or intermittency bifurcation.[20,21] There the varying control parameter is mainly the residence time τ, and P_1^m, $m = 1, 2, 3, 4...$ are located in relatively small τ regime. It was found that between each P_1^m and P_1^{m+1}, there is a chaotic region of comparable range and this kind of alternating periodic-chaotic sequence seems reminiscent of dynamic behaviors involving a homoclinic orbit.[22,23] This is different from our system in which, if the transitions from P_1^m to P_1^{m+2} are indirect at all, the intermediate region must be extremely small.

We remark that varying the residence time in addition to P and T_0 will likely to be very relevant for the studies of bifurcations. Besides, with three external control parameters, it would be promising to approach bifurcations of higher codimension around which complex aperiodic behavior could be generated.

The extreme sensitivity of the system to temperature may make experimental studies of detailed bifurcation cascading in region III difficult to achieve. It would be very interesting if further theoretical analysis could indicate how to enlarge the region III by either physical or chemical means, and thereby provide concrete indication for the experimental search of those interesting dynamic behaviors.

ACKNOWLEDGMENTS

The authors are sincerely grateful to Professor G. Nicolis for suggesting the problem and stimulating discussions; to Professor P. Gray, Professor J. F. Griffiths, and Professor R. Ben-Aïm for helpful communications on their works. C. Y. Mou thanks Profesor I. Prigogine for kind hospitality and support during his stay at Bruxelles, and the National Science Council for a sabbatical leave grant. This research is supported, in part, by the U. S. Department of Energy under contract number DE-AS05-81ER10947.

[1] P. Gray, J. F. Griffits, S. M. Hasko, and P. G. Lignola, Proc. R. Soc. London Ser. A **374**, 313 (1981).
[2] A. D. Walsh, *Ninth International Symposium on Combustion* (Academic, New York, 1963), p. 1046.
[3] *Chemical Instabilities*, edited by G. Nicolis and F. Baras, NATO ASI Series C120 (Reidel, Dordrecht, 1984).
[4] A recent account is given in *Order in Chaos*, Physica D **7**, Nos. 1–3 (1983).
[5] For a review, see I. R. Epstein, J. Phys. Chem. **88**, 187 (1984).
[6] R. J. Field and R. M. Noyes, J. Chem. Phys. **60**, 1877 (1974).
[7] M. P. Halstead, A. Prothero, and C. P. Quinn, Proc. R. Soc. London Ser. A **322**, 377 (1971).
[8] M. P. Halstead, A. Prothero, and C. P. Quinn, Combust. Flame **20**, 211 (1973).
[9] P. G. Felton, B. F. Gray, and N. Shank, Combust. Flame **27**, 363 (1976).
[10] C. Gibson, P. Gray, J. F. Griffiths, and S. M. Hasko, in Twentieth Symposium on Combustion, The Combustion Institute (1984).
[11] H. Davy, Philos. Trans. R. Soc. London **107**, 77 (1817).
[12] B. F. Gray and C. H. Yang, J. Phys. Chem. **69**, 2747 (1965); C. H. Yang and B. F. Gray, *ibid.* **73**, 339 (1969).
[13] I. E. Salnikoff, Zh. Fiz. Khim. **23**, 258 (1949).
[14] L. P. Blanchard, J. B. Farmer, and C. Ouellet, Can. J. Chem. **35**, 115 (1957).
[15] I. Gonda and B. F. Gray, Proc. R. Soc. London Ser. A **389**, 133 (1983).
[16] I. Gonda and B. F. Gray, J. Chem. Soc. Faraday Trans. **2**, 1729 (1983).
[17] H. Rabitz, M. Kramer, and D. Dacol, Annu. Rev. Phys. Chem. **34**, 419 (1983).
[18] J. L. Hudson, M. Hart, and D. Marinko, J. Chem. Phys. **71**, 1601 (1979).
[19] J. S. Turner, J. C. Roux, W. D. McCormick, and H. L. Swinney, Phys. Lett. A **85**, 9 (1981).
[20] R. H. Simoyi, A. Wolf, and H. L. Swinney, Phys. Rev. Lett. **49**, 245 (1982).
[21] Y. Pomeau, J. C. Roux, A. Rossi, S. Bachelart, and C. Vidal, J. Phys. Lett. **42**, L271 (1981).
[22] P. Glendinning and C. Sparrow, J. Stat. Phys. **35**, 645 (1984).
[23] P. Gaspard, R. Kapral, and G. Nicolis, J. Stat. Phys. **35**, 697 (1984).